Metabolic profiles of dystrophin and utrophin expression in mouse models of Duchenne muscular dystrophy

J.L. Griffin[a,*], E. Sang[b], T. Evens[a], K. Davies[c], K. Clarke[b]

[a] *Biological Chemistry, Biomedical Sciences, Faculty of Medicine, Imperial College of Science, Technology and Medicine, London SW7 2AZ, UK*
[b] *Department of Biochemistry, University of Oxford, Oxford OX1 3QU, UK*
[c] *Department of Human Anatomy and Genetics, University of Oxford, Oxford OX1 3QU, UK*

Received 16 July 2002; revised 12 August 2002; accepted 27 August 2002

First published online 20 September 2002

Edited by Thomas L. James

Abstract Metabolic profiles from ^{1}H nuclear magnetic resonance spectroscopy have been used to describe both one and two protein systems in four mouse models related to Duchenne muscular dystrophy using the pattern recognition technique partial least squares. Robust statistical models were built for extracts and intact cardiac tissue, distinguishing mice according to expression of dystrophin. Using metabolic profiles of diaphragm, models were built describing dystrophin and utrophin, a dystrophin related protein, expression. Increased utrophin expression counteracted some of the deficits associated with dystrophic tissue. This suggests the method may be ideal for following treatment regimes such as gene therapy.

Key words: Dystrophin; Utrophin; Duchenne muscular dystrophy; Metabolomics; Metabolic profile

1. Introduction

Duchenne muscular dystrophy (DMD) is an X-linked recessive disorder characterised by progressive muscle wasting, leading to death from pulmonary or cardiac complications [1]. Dystrophin, a 427 kDa costameric protein, binds the actin cytoskeleton and links it to the extracellular matrix by associating with a large transmembrane glycoprotein complex [2–5]. This dystrophin–glycoprotein complex is thought to play a role in sarcolemmal stabilisation during the contraction cycle, as absence of dystrophin renders the sarcolemma susceptible to contraction induced injury.

Utrophin is functionally analogous to dystrophin, with both proteins possessing binding sites for actin and the dystrophin–glycoprotein complex, albeit through different motifs [6]. The protein is found over the entire surface of muscle fibres in foetal skeletal muscle, but is replaced by dystrophin during development, when utrophin becomes localised to the neuromuscular junction in adult skeletal muscle [7–9]. The dystrophic phenotype normally observed in *mdx* mice, a model of DMD, is absent when muscles overexpress utrophin [10–12].

Attempts to replace the missing mutated dystrophin gene using transgene therapy have proven difficult, and are complicated by the immune reaction generated by expressing dystrophin, a protein seen as foreign to a patient who does not possess a functional copy of the gene [13]. For this reason upregulation of utrophin expression in muscle is a favoured gene therapy approach for DMD.

We have previously shown using a combination of pattern recognition and either solution or solid state ^{1}H nuclear magnetic resonance (NMR) spectroscopy that muscle and brain tissue from *mdx* mice have distinct metabolic profiles compared with control animals [14,15]. These studies used principal component analysis (PCA), an unsupervised method of pattern recognition, to classify tissues according to metabolic profiles.

The aim of this study was to investigate the metabolic profiles of cardiac and diaphragm tissue from four different mouse models, all expressed on the same C57BL/10 background: (i) the *mdx* mouse which does not express dystrophin; (ii) Tg/Dmd^{mdx}: transgenic mouse expressing full-length utrophin in skeletal muscle but not heart crossed with the *mdx* mouse to produce mice lacking dystrophin but having utrophin localised at the sarcolemma [11]; (iii) $Tg_{truncated}/Dmd^{mdx};utrn^{-/-}$: transgenic mice expressing a truncated utrophin transgene crossed onto a $Dmd^{mdx}/utrn^{-/-}$ double mutant background, resulting in a mouse with no dystrophin in skeletal muscle but with a truncated utrophin transgene and heart with no dystrophin or utrophin [16]; (iv) the control mice to (iii), $Tg_{truncated}/Dmd^{mdx}$, which have no dystrophin but express utrophin. Prediction to latent structures through partial least squares (PLS [17]) was used to correlate protein expression with metabolic profiles. We show that distinct metabolic profiles are associated with the expression of dystrophin and utrophin. Furthermore, this is a general approach suitable for the investigation of other protein system.

2. Materials and methods

2.1. Materials

All mice were maintained according to the UK Home Office guidelines. Male 6 month old mice were removed from stable colonies of C57BL/10 control mice ($n=8$ for cardiac tissue, 10 for aqueous extracts, 5 for diaphragm), *mdx* ($n=12$ for heart, 5 for diaphragm), Tg/Dmd^{mdx} ($n=5$); $Tg_{truncated}/Dmd^{mdx};utrn^{-/-}$ ($n=2$ for heart) and $Tg_{truncated}/Dmd^{mdx}$ ($n=2$ heart) mice (Table 1). Animals were killed by cervical dislocation, and cardiac and diaphragm tissues were removed rapidly. Tissue was immediately frozen in liquid nitrogen and stored for no longer than 24 h at −40°C prior to NMR analysis. Genetic integrity of the colonies was monitored throughout.

2.2. Methods

Frozen cardiac and diaphragm tissues were pulverised using a pestle

*Corresponding author. Fax: (44)-20-7594 3226.
E-mail address: j.griffin@ic.ac.uk (J.L. Griffin).

0014-5793/02/$22.00
PII: S0014-5793(02)03437-3

Table 1
Summary of mouse models used in this study

Mouse strain	Heart		Skeletal muscle and diaphragm		Phenotype
	Dys	Utr	Dys	Utr	
C57BL/10 control	+	+	+	+	Normal
Mdx	−	+	−	+	Mild cardiac hypertrophy, ~60% centrally nucleated fibres in diaphragm
Tg/Dmd^{mdx}	−	+	−	++	No difference from control tissue
$Tg_{truncated}/DMD^{mdx}$	−	+	−	++	Some increase in centrally nucleated fibres in skeletal muscles and diaphragm
$Tg_{truncated}/Dmd^{mdx};utrn^{-/-}$	−	−	−	+ (trun)	Marked myopathy, premature death, connective tissue proliferation, waddling gait, arched spine

Phenotype information is from [11,12,31]. Dystrophin (dys) and utrophin (utr) expression are measured in relative terms: + normal expression, ++ increased, − decreased, trun truncated.

and mortar, and metabolites extracted with a 1:1 mixture of acetonitrile and water (100 mg in 1 ml). The solvent was lyophilised and extracts redissolved in D_2O. All spectra were acquired in a 14.1 T superconducting magnet interfaced to an AVANCE spectrometer (Bruker, Karlsruhe, Germany). Solvent suppressed spectra were acquired into 16k data points, averaged over 128 scans, using a pulse sequence based on the start of a NOESY pulse sequence (relaxation delay = 1.5 s, mixing time = 150 ms).

For solid state spectra of cardiac tissue, 10 mg of tissue was soaked in D_2O and packed into zirconium oxide rotors, with 5 μl of D_2O and 10 mM 2,2,3,3-D trimethylsilyyl, 1-propionic acid (TSP), using a rotor spacer to ensure packing homogeneity. The rotors were spun at 5000 Hz at 300 K in a high resolution magic angle spinning (HRMAS) probe placed in the spectrometer described above. Spectra were acquired using the solvent suppressed sequence described above. Free induction decays were collected into 16k data points and averaged over 256 scans. Carr Purcell Meiboom and Gill (CPMG) spectra were also acquired using a 40 ms total spin echo delay with 40 spin echoes each of 500 μs between the π pulses. Continuous wave irradiation was used to suppress the water resonance. Other parameters were identical to those used with the solvent suppressed spectra described above.

All spectra were processed using XWINNMR software (version 3.1; Bruker). Following multiplication by either a 0.3 or 1 Hz exponential function for liquid and solid state spectra, respectively, spectra were Fourier transformed from the time to frequency domain, phased and baseline corrected.

2.3. Pattern recognition of tissue spectra

Spectra were integrated across 0.04 ppm spectral regions between 0.4 and either 4.2 or 9.4 ppm for solid and solution state NMR, respectively, using the AMIX software package (Bruker). The output vector representing each spectrum was normalised across the integral regions, excluding the water resonance. Data sets were imported into the SIMCA package (Umetrics, Umeå, Sweden) and then preprocessed using three different scaling processes: (i) mean centring by measuring the variance of each integral region about this mean, (ii) univariate using mean centring followed by scaling the variance by $1/s_k$ where s is the standard deviation of the variable (integral region) k and (iii) Pareto scaled to $(1/s_k)^{1/2}$.

Each integral region represented an X variable in the PLS model. Protein expression was represented as a Y vector. For both tissue types presence and absence of dystrophin was represented as 1 or 0 (expression or failure). For diaphragm tissue, utrophin expression was represented by a second Y variable as 1 (normal expression) or 2 (promoted expression). The goodness of fit algorithm was used to determine whether a correlation was significant ($Q^2 > 0.097$), and how many PLS components were used in the model. Metabolic perturbations caused by a failure to express a protein were determined from loadings plots. Spectral regions having a modulus loadings score of greater than 50% of the maximum loading value for that model were identified as having the most significant changes.

3. Results

Three data matrices were prepared using the cardiac tissue from the five mouse strains: one derived from aqueous extracts and two investigating intact tissue. Of the two HRMAS ^{1}H NMR spectroscopy pulse sequences used, the CPMG experiment, relying on T_2 attenuation of the FID, produced spectra with most contributions from low molecular weight metabolites while the solvent suppressed spectra were dominated by lipid resonances (Fig. 1A). The three matrices represented a graduated change in environment from lipophilic to hydrophilic. By visual inspection the spectra could not be separated into the five groups of animals for either of the three pulse sequences, indicating that failure to express dystrophin does not induce a major metabolic perturbation.

Using the solvent suppressed spectra from intact cardiac tissue, two PLS models were built, using either univariate or Pareto prescaling, correlating dystrophin expression to the metabolic profile for the five different mouse types (Fig. 1B; Table 2). Pareto preprocessing identified five resonance regions as being increased and seven regions as decreased in relative spectral intensity following the expression of dystrophin. These resonance regions were all represented in the univariate model, along with three further regions of increased and two regions of decreased spectral intensities. Examining the spectra, these resonance regions correlated with an increase in lipid moieties, taurine and creatine and a decrease in glucose and β-hydroxybutyrate in dystrophic tissue (Table 2).

The CPMG matrix was employed to investigate motionally less restrained metabolites in the intact tissue. Using all three methods of preprocessing, a one component model was formed from the spectral intensities using the CPMG pulse sequence as the X matrix and dystrophin expression as the Y vector ($Q^2 = 0.102$ (mean centred); $Q^2 = 0.169$ (Pareto; Fig. 1B(2)); $Q^2 = 0.197$ (univariate)). A total of 15 spectral regions were found to contribute to at least 50% of the maximum loadings score across the three models (Table 2).

The aqueous extract spectral matrix was most discriminating in terms of dystrophin expression. All three preprocessing routines gave significant models for a PLS analysis of the metabolic profiles in terms of protein expression. Both univariate ($Q^2 = 0.181$) and Pareto ($Q^2 = 0.230$; Fig. 1B(3)) preprocessing produced PLS models with one component, while mean centred preprocessing produced a two component model (cumulative $Q^2 = 0.509$). In total 22 spectral regions were identified as contributing to the separation at 50% or greater of the maximum loadings contribution. In keeping with the mathematical basis of the three preprocessing techniques, Pareto scaling provided a half way point between the two extremes of no scaling and univariate scaling. Intriguingly, one

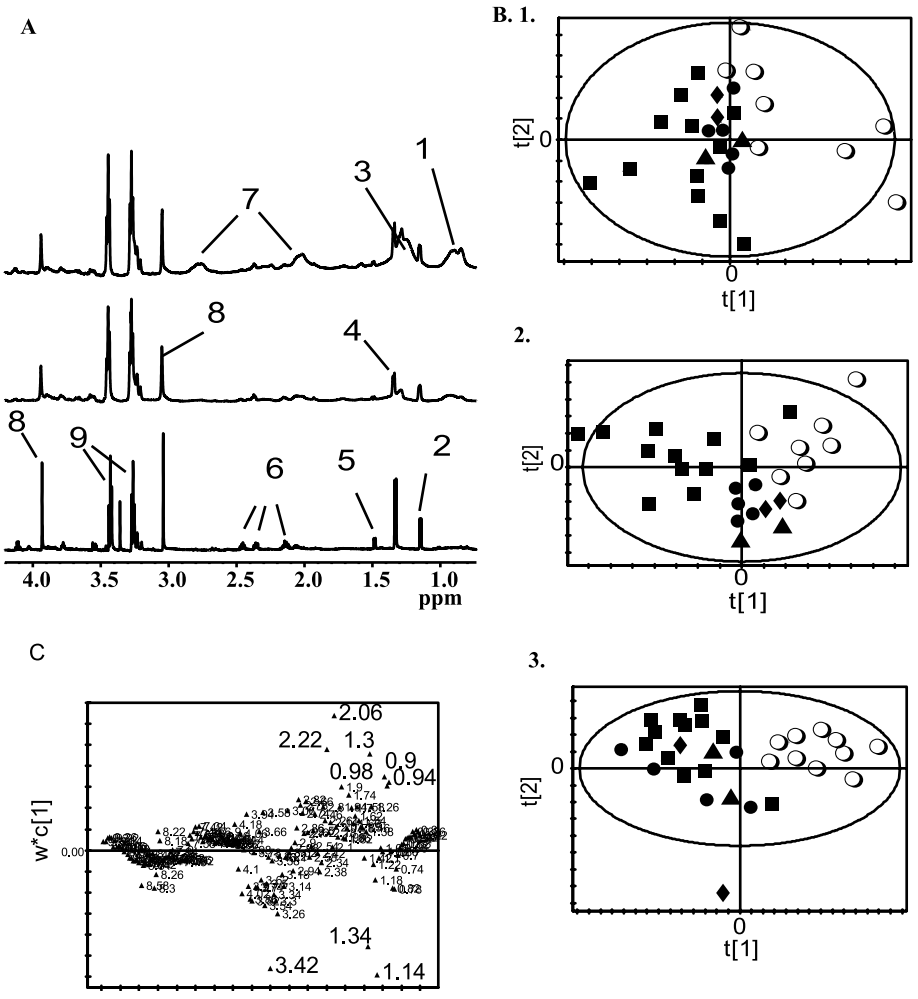

Fig. 1. Intact tissue and aqueous extracts of cardiac tissue were investigated by ^{1}H NMR spectroscopy. Three data matrices were formed from high resolution spectra (A) taken from intact tissue using either a standard pulse and acquire sequence (top) or a T_2 edited pulse sequence with a total relaxation time of 40 ms (middle), or from acetonitrile/water extracts of the tissue (bottom). PLS regression models were built (B; all with Pareto prescaling) modelling expression of changes in metabolic profile against dystrophin expression. The loadings plots (C) for these models were used to distinguish which metabolites were the most significant in terms of describing this separation. Key: 1. CH_3CH_2– lipid groups, 2. β-hydroxybutyrate, 3. CH_2CH_2 lipid, 4. lactate, 5. alanine, 6. glutamate, 7. $CH_2CH_2CH{=}CH$ lipid groups, 8. creatine, 9. taurine. ○ control; ■ *mdx*; ● Tg/Dmd^{mdx}; ♦ $Tg/Dmd^{mdx};utrn^{-/-}$; ▲ $Tg_{truncated}/DMD^{mdx}$.

metabolite, β-hydroxybutyrate, was consistently decreased in dystrophic intact cardiac tissue but increased in the aqueous extract, suggesting an 'NMR invisible pool', possibly mitochondrial.

To further examine the Pareto preprocessed data set a series of further models were built. Orthogonal signal correction (OSC) was applied using dystrophin expression as the Y vector for this data filtering technique. Extracting two components of data not correlated to dystrophin expression produced a data set representing 33% of the remaining variation. Using this data set, a PLS model was built correlated to protein expression, with a goodness of fit algorithm of $Q^2 = 0.875$, explaining 47% of the remaining spectral variation and 97% of the variation produced in mapping protein expression to $Y = 0$ or 1. In addition to the metabolites identified in the pre-OSC filtered data set, two further regions were identified ($\delta = 3.06$, 3.94) corresponding to creatine. Applying PCA to the OSC filtered data set, separation was most apparent in the first two components which represented 93% of the remaining spectral variation and a goodness of fit of $Q^2 = 0.682$ (Fig. 2). Spectral regions identical to the PLS analysis were identified as contributing significantly to the separation.

To test model robustness, PLS was used to predict dystrophin expression in a subset of the extract spectra. The data set was preprocessed using Pareto scaling, and random selections of spectra were excluded for four different models (six out of the 31 spectra). The resulting PLS models had a combined success rate of 96 ± 7% (equivalent to one incorrectly assigned spectrum out of the four models). To examine how the technique would predict new mouse models for DMD, Tg/Dmd^{mdx} and a combination of $Tg_{truncated}/Dmd^{mdx};utrn^{-/-}$ and $Tg_{truncated}/Dmd^{mdx}$ were excluded separately from different PLS models built using the remainder of the data (26 and 27 spectra, respectively), with the prediction success being 80% and 75%, respectively (in both cases one spectrum was misclassified in each model built). The mean Y PLS scores for Tg/Dmd^{mdx} were 0.22 ± 0.18, and for $Tg_{truncated}/Dmd^{mdx};utrn^{-/-}$ and $Tg_{truncated}/Dmd^{mdx}$ 0.32 ± 0.13.

3.1. Building a two component model for the diaphragm

Having shown that failure to express dystrophin was asso-

Table 2
Metabolites increased or decreased in dystrophic cardiac tissue compared to the normal group for the PLS models built

Pulse sequence	Scaling of data	Q^2	Metabolites increased	Metabolites decreased
HRMAS solvent suppress	Univariate	0.26	CH_3CH_2 lipid (1.0), lactate, (1.34), $CH_2C=C$ (2.1–2.0), glutamate (2.36), $C=CCH_2C=C$ (2.78), lysine (3.02), taurine (3.26, 3.46)	Glucose (3.5–3.86), choline (3.20), malonate (3.13), β-hydroxybutyrate (1.20), cholesterol (0.78)
	Pareto	0.34	Taurine (3.26, 3.46), $CH_2C=C$ (2.1–2.0), lactate (1.34), CH_3CH_2 lipid (0.9)	Choline (3.20), malonate (3.13), β-hydroxybutyrate (1.20), cholesterol (0.78)
	Mean centred	No fit		
HRMAS CPMG	Univariate	0.30	$CH_2C=C$ (2.1–2.0), CH_2CH_2CO (1.58), lactate (1.34, 4.14), $CH_2CH_2CH_2$ lipids (1.32–1.27), CH_3CH_2 lipids (0.90)	Glucose (3.50–3.70), α-ketoglutarate (2.45), acetate (1.94), $CH_2CH_2C=C$ (1.74–1.70), β-hydroxybutyrate (1.20)
	Pareto	0.43	Taurine (3.26), glutamate (2.38), lactate (1.34)	β-Hydroxybutyrate (1.16)
	Mean centred	0.10	Taurine (3.26), lactate (1.34)	
Aqueous extract	Univariate	0.18	ATP (8.58), inosine (8.3), glycerol (4.02, 3.56), β-hydroxybutyrate (1.16), *n*-butyrate (0.90)	Dimethylglycine (2.82), aspartate (2.68), glutamine (2.22, 2.10), acetate (1.90), leucine (1.70), lysine (1.74), leucine, isoleucine, valine (0.98–0.94)
	Pareto	0.23	Taurine (3.42), lactate (1.34), β-hydroxybutyrate (1.16)	Glutamine (2.22), glutamate (2.06), isoleucine/leucine (0.94–0.98)
	Mean centred	0.51	Taurine (3.42), lactate (1.34), β-hydroxybutyrate (1.16)	Creatine (3.06, 3.94), glutamate (2.06)

Chemical shifts are shown in parentheses.

ciated with a distinct metabolic profile in the heart across four mouse models of the disease, we examined a two protein system in C57BL/10 control, *mdx* and Tg/Dmd^{mdx} mice. The effects of dystrophin and utrophin expression on metabolic profile were examined in extracts of diaphragm tissue. Dystrophin expression was modelled as 1 (present) or 0 (absent) and utrophin expression as 1 (normal expression) or 2 (promoted expression). Two component PLS models were built separating the data group into the three mouse groups (goodness of fit $Q^2 = 0.295$ (univariate), 0.412 (Pareto; Fig. 3), 0.402 (mean centred)). Using the Pareto model, the mean second PLS component loadings (±S.E.M.), corresponding most closely to distinguishing dystrophic tissue, for each mouse type were significantly different for *mdx* and control mice according to an ANOVA test of variance followed by a Tukey Kramer post test, but placed Tg/Dmd^{mdx} as intermediate ($mdx = -8.7 \pm 1.2$, control $= 7.5 \pm 4.2$, $Tg/Dmd^{mdx} = 1.5 \pm 2.8$; $P < 0.01$ for differences between control and *mdx*).

Fig. 2. The data filtering technique OSC was successful in removing variation in the data not attributable to dystrophin expression in the cardiac tissue. Following OSC, the three data matrices from the cardiac tissue could be readily separated according to dystrophin expression by PCA. Similar metabolites to those identified using PLS were observed to contribute to the loadings. A: PCA of aqueous extract matrix for cardiac tissue. B: Accompanying loadings plot to PCA. Key: as above.

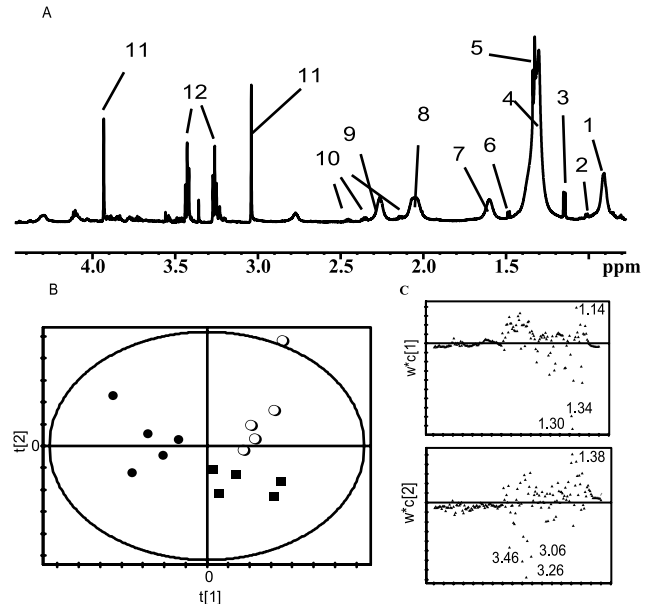

Fig. 3. A two component PLS model was built to examine the metabolic profile of diaphragm tissue in terms of dystrophin and utrophin expression. A: High resolution ^{1}H NMR spectra of aqueous extracts were used as the X inputs to the PLS model. The acetonitrile/water mixture also extracted small chain lipids. B: A two component PLS model (Pareto scaled data shown). C: Loadings plots were derived for utrophin (top) and dystrophin (bottom) showing which metabolites contributed most to the model. Key: 1. CH_3CH_2 lipid, 2. leucine, valine and isoleucine, 3. β-hydroxybutyrate, 4. CH_2CH_2 lipids, 5. lactate, 6. alanine, 7. CH_2CH_2CO lipid groups, 8. $CH_2CH_2CH{=}CH$, 9. $CH_2CH{=}CH$ lipid, 10. glutamate, 11. creatine, 12. taurine. ○ control; ■ *mdx*; ● *Tg/Dmd*^{mdx}.

The loadings score for each PLS component indicated the key metabolites perturbed by a change in protein expression. The upregulated utrophin expression in *Tg/Dmd*^{mdx} mice showed decreased concentrations of glycerol, creatine and glucose and increased concentrations of short chain fatty acids and β-hydroxybutyrate in diaphragm tissue (Table 3). Again, as in cardiac tissue, taurine appeared to be a significant biomarker for dystrophin expression. Examining contribution scores for the PLS component modelling dystrophin expression, tissue extracts from *Tg/Dmd*^{mdx} mice demonstrated metabolic profiles intermediate between the control and *mdx* mouse. This suggests that promoting utrophin expression can negate the metabolic effects of a failure to express dystrophin.

3.2. Temporal progression of metabolites in mdx and control mice

The above PLS models were all built using spectra from animals aged ~6 months old. However, metabolite pool sizes also vary with development and during ageing. Thus, spectral variation with age was investigated in tissue extracts from C57BL/10 control and *mdx* mice using PLS with Pareto scaling ($n=3$ for 3, 6, 10 and 15 month ages). For both diaphragm and cardiac tissue one component models were built indicating that for both mouse strains there was a temporal progression in metabolites (Fig. 4). However, this progression was different between strains. In cardiac and diaphragm tissue from *mdx* mice, the concentrations of β-hydroxybutyrate, creatine and taurine resonances decreased and lactate increased with age. The age related changes were less defined in control

Table 3
Metabolites are shown that are increased or decreased in dystrophic tissue and that are increased or decreased by increased utrophin expression in diaphragm tissue

PLS model	Q^2	R^2X	Dystrophin component	Utrophin component
Univariate	0.30	0.70	Increased: ATP (8.58), inosine (8.3), taurine (3.42, 3.26), short chain CH_2CO lipid (2.38), $CH_2C{=}C$ lipid (2.10), creatine (3.06, 3.94), glycerol (4.1) Decreased: Short chain $C{=}CCH_2C{=}C$ lipid, acetate (1.93), short chain CH_2CH_2CO lipid, β-hydroxybutyrate (1.16)	Increased: Short chain fatty acids (2.80–2.72), glutamate (2.34), short chain $CH_2C{=}C$ fatty acids (2.02), CH_2CH_2CO short chain fatty acid Decreased: Glycerol (4.02), betaine (3.90), glucose (3.82, 3.62, 3.46),
Pareto	0.41	0.67	Increased: Taurine (3.26, 3.42), creatine (3.06, 3.96)/C >< br>Decreased: Short chain $CH_2CH_2CH_2$ lipids (1.30)	Increased: Lactate (1.34), short chain CH_3CH_2 lipid Decreased: β-Hydroxybutyrate (1.16)
Mean centred	0.40	0.78	Increased: Taurine (3.42, 3.26), creatine (3.06, 3.94), lactate Decreased: Alanine (1.45)	Increased: lactate (1.34)

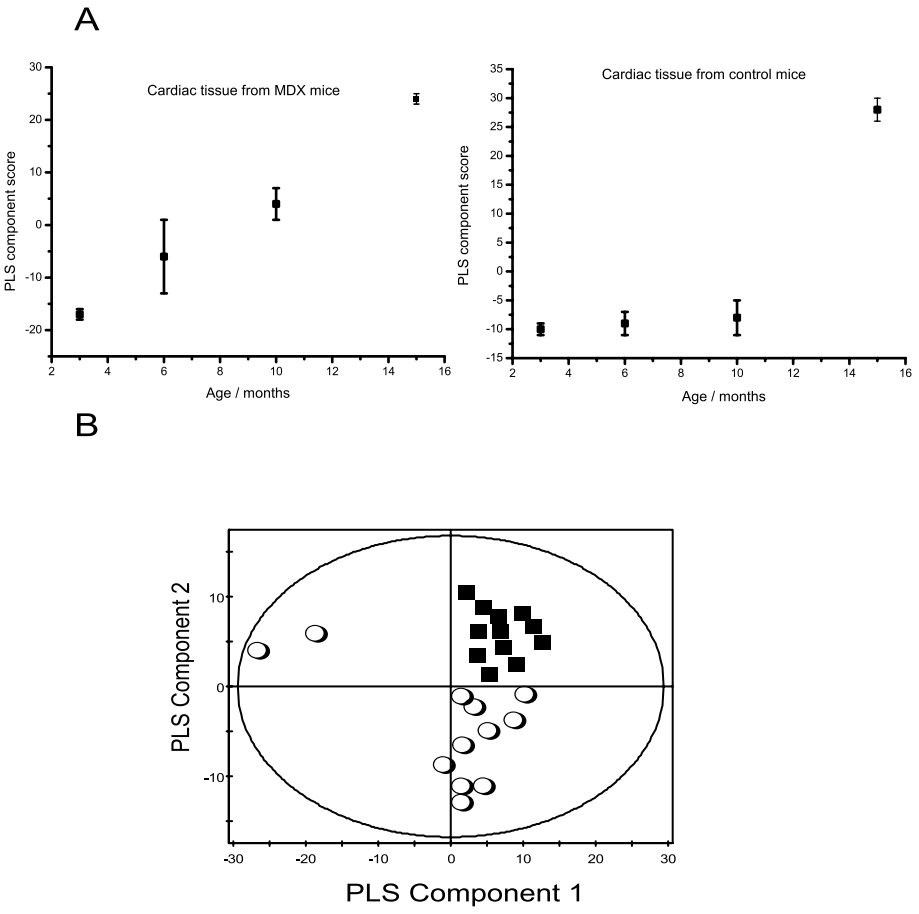

Fig. 4. A: PLS models were built to examine age related metabolite changes in extracts of cardiac tissue from *mdx* and C57BL/10 control mice between 3 and 15 months. Each point represents the mean PLS score ± S.D. ($n = 3$). Plotted against time, the PLS scores for dystrophic tissue displayed an almost linear response, while the PLS scores in control tissue from 15 month old animals displayed the largest perturbation. B: Despite these changes control (○) and dystrophic (■) tissue can be readily distinguished using PCA or PLS (shown). The two control spectra found in the most extreme left of the plot are from 15 month old animals.

spectra, as determined by the contribution scores of individual metabolites and the Q^2 of the model, and were caused by a decrease in lactate and an increase in glucose concentrations with age. However, for all the spectra from a given strain, the differences between strain were greater than those caused by age as measured by PCA or PLS techniques (Fig. 4), with dystrophic tissue having an increased concentration of taurine and a decrease in creatine.

4. Discussion

Somatic manipulation of the genome of models of DMD has produced poor results, and current treatment strategies have focused on upregulating DRP proteins to compensate for the missing dystrophin. Central to these strategies is an understanding of gene expressions in terms of their functional responses. This is a particular challenge for the *mdx* mouse, and related models, where the disease phenotype is mild in comparison to humans. In this study we have used PLS, a supervised pattern recognition technique, to perform regressions between metabolic profile and protein expression in cardiac and diaphragm tissue. Despite their different genotype a common metabolic deficit was identified across the mouse models used in this study.

Although not primarily a metabolic disorder, dystrophic muscle tissue is characterised by perturbed metabolism [18–21]. We have previously demonstrated using PCA of ^{1}H NMR spectra of tissue extracts that a range of tissues from *mdx* mice have distinct metabolic profiles compared to control siblings both in tissue extracts [14] and in intact cardiac tissue [15]. Many of the metabolites identified as being altered in cardiac tissue have been identified previously using PCA of *mdx* tissue alone, including an increase in lipid chain length, increased concentration of the non-polar amino acids leucine, valine and isoleucine and an increased concentration of taurine. The concentration of taurine has also been previously correlated with muscle regeneration following necrosis [20,21]. However, a number of metabolites had not previously been identified, including *n*-butyrate and glycerol, indicative of a failure to process ketone bodies and fatty acid derivatives. Unlike the classification tool PCA, this approach could also be used to predict gene expression. Using the data set derived from cardiac tissue extracts we were able to demonstrate that models could be built capable of classifying test data, even for new mouse models of the disease that had not been included in the building of the model.

Tg/Dmd^{mdx} mice do not express dystrophin, but have promoted utrophin expression in skeletal muscle and diaphragm (but not cardiac muscle). This allowed the formation of a PLS model where two proteins were correlated with metabolic phe-

notype. Control and *mdx* diaphragm tissue was readily separated across one PLS component caused by a series of changes including an increase in the concentration of taurine. The increased utrophin expression in *Tg/Dmd*^{mdx} mice also influenced small molecule metabolism, with diaphragm tissue having increased concentrations of lactate and alanine compared with both *mdx* and control diaphragm tissue.

However, more intriguingly the mean scores for the PLS component correlated to dystrophin expression for *Tg/Dmd*^{mdx} diaphragm tissue was intermediate between the *mdx* and control mouse tissue. The first wave of muscle necrosis only occurs in dystrophic tissue when utrophin expression falls below that found in neonatal muscle. Tinsley and co-workers [11] have demonstrated that increased utrophin expression reverses the phenotype characteristic of *mdx* mouse muscle tissue. In our study we have also found evidence of the beneficial action of promoted utrophin expression in dystrophic tissue in terms of the metabolic phenotype produced. A number of treatments for DMD have been suggested, including temporary changes in protein expression [22–24], aminoglycosides that suppress stop mutations [25], the introduction of stem cells [26] or the targeting of promoter and enhancer regions of the utrophin gene [27–29]. PLS derived metabolic profiles may be used for screening other potential molecular activating factors. Although the field strengths used in this study are higher than that used in clinical systems, 9.4 and 11.7 T experimental in vivo systems are increasingly common for studying mice and rats. Alternatively, human muscle tissue removed by biopsy may be monitored using HRMAS ^{1}H NMR spectroscopy as described in this study.

The techniques described in this study may be useful for following a range of protein changes as measured by proteomics. There are a number of dystrophin related proteins other than utrophin, and the failure to express dystrophin also affects expression of proteins in the dystrophin–glycoprotein complex. With further animal models of related disorders [30] the action of dystrophin related proteins and dystrophin–glycoprotein complex proteins could be modelled in terms of metabolic phenotypes. In addition, mouse models of Beckers muscular dystrophy could be examined to investigate the effects of impaired dystrophin expression, rather than lack of expression. The inclusion of a model of cardiac hypertrophy may also shed light on the mechanisms involved in muscle failure in the *mdx* mouse. Although cardiac hypertrophy is mild at 6 months in *mdx* mice [31], some of the metabolic changes detected at this time point may be indicative of the early stages of this disease. However, by using four different models of DMD, each with different severities of cardiac and muscular abnormalities, the metabolic changes detected appear associated with dystrophin and utrophin expression rather than cardiac hypertrophy or cellular proliferation after necrosis. McIntosh and co-workers have previously correlated cardiac taurine concentrations with regeneration and myogenic cell proliferation in *mdx* mice, mice deficient in the early myogenic regulatory gene (MyoD) and the double mutant *mdx*:MyoD(−/−) cross strain [20]. While no 'omic' approach can separate the causes and consequences of a phenotype from the transcriptome, proteome or metabolon, it may be possible to use related mouse models to interrogate which pathways are common to given events such as muscular hypertrophy [31–33], cellular proliferation and muscle repair [20,21,34] and muscular denervation and reinnervation [35]. For such studies metabolomics provides a cheaper alternative to transcriptomics and proteomics.

The techniques used in our study are not confined to this application, or mammalian systems. Such metabonomic/metabolomic approaches have been used in the study of drug toxicology [36], probing 'silent phenotypes' in yeast cells [37], or alternatively, the already characterised *Caenorhabditis elegans* model of DMD [38], where the dystrophin analogue dys-1 has been knocked out, could be used to screen for small molecules which promote upregulation of dystrophin related proteins in this animal.

In conclusion, we have demonstrated that a failure to express dystrophin in cardiac and diaphragm muscle produces metabolic phenotypes distinct to the protein, and this may be used to characterise new models of the disease. These models also predict that increased utrophin expression may prevent some of the metabolic deficits associated with dystrophic tissue.

Acknowledgements: This work was supported by the Royal Society (J.L.G.) and the British Heart Foundation (E.S., K.D. and K.C.). J.L.G. also acknowledges Professor J.K. Nicholson for generous access to NMR spectrometers.

References

[1] Emery, A.E.H. (1990) Neuromusc. Disord. 1, 19–29.
[2] Hoffman, E.P., Brown Jr., R.H. and Kunkel, L.M. (1987) Cell 51, 919–928.
[3] Koenig, M., Monaco, A.P. and Kunkel, L.M. (1988) Cell 53, 219–226.
[4] Tinsley, J.M., Blake, D.J. and Roche, A. et al. (1992) Nature 360, 591–593.
[5] Ahn, A.H. and Kunkel, L.M. (1993) Nature Genet. 4, 283–291.
[6] Rybakova, I.N., Patel, J.R., Davies, K.E., Yurchenco, P.F. and Ervasti, J.M. (2002) Mol. Biol. Cell 13, 1512–1521.
[7] Hoffman, E.P., Beggs, A.H., Koeni, gM., Kunkel, L.M. and Angelini, C. (1989) Lancet 2, 1211–1212.
[8] Khurana, T.S., Hoffman, E.P. and Kunkel, L.M. (1990) J. Biol. Chem. 265, 16717–16720.
[9] Khurana, T.S., Watkins, S.C. and Chafey, P. et al. (1991) Neuromusc. Disord. 1, 185–194.
[10] Tinsley, J.M., Potter, A.C., Phelps, S.R., Fisher, R., Trickett, J.L. and Davies, K.E. (1996) Nature 384, 349–353.
[11] Tinsley, J., Deconinck, N., Fisher, R., Kahn, D., Phelps, S., Gillis, J.M. and Davies, K. (1998) Nature Med. 4, 1441–1444.
[12] Deconinck, N., Tinsley, J., De Backer, F., Fisher, R., Kahn, D., Phelps, S., Davies, K. and Gillis, J.M. (1997) Nature Med. 3, 1216–1221.
[13] Burton, E. and Davies, K. (2002) Cell 108, 5–8.
[14] Griffin, J.L., Williams, H.J., Sang, E., Clarke, K., Rae, C. and Nicholson, J.K. (2001) Anal. Biochem. 293, 16–21.
[15] Griffin, J.L., Williams, H.J., Sang, E. and Nicholson, J.K. (2001) Magn. Reson. Med. 46, 249–255.
[16] Rafael, J.A., Tinsley, J.M., Deconinck, A.E. and Davies, K.E. (1998) Nature Genet. 19, 79–82.
[17] Eriksson, L., Johansson, E., Kettaneh-Wold, N. and Wold, S. (1999) Introduction to Multi- and Megavariate Data Analysis using Projection Methods (PCA and PLS). Umetrics, Umeå.
[18] Kemp, G.J., Taylor, D.J., Dunn, J.F., Frostick, S.P. and Radda, G.K. (1993) J. Neurol. Sci. 116, 201–206.
[19] Even, P.C., Decrouy, A. and Chinet, A. (1994) Biochem. J. 304, 649–654.
[20] McIntosh, L.M., Garrett, K.L., Megeney, L., Rudnicki, M.A. and Anderson, J.E. (1998) Anat. Rec. 252, 311–324.
[21] McIntosh, L.M., Baker, R.E. and Anderson, J.E. (1998) Biochem. Cell Biol. 76, 532–541.
[22] Krag, T.O., Gyrd-Hansen, M. and Khurana, T.S. (2001) Acta Physiol. Scand. 171, 349–358.
[23] Cordier, L., Hack, A.A., Scott, M.O., Barton-Davis, E.R., Gao,

G., Wilson, J.M., McNally, E.M. and Sweeney, H.L. (2000) Mol. Ther. 1, 119–129.
[24] Wang, B., Li, J. and Xiao, X. (2000) Proc. Natl. Acad. Sci. USA 97, 13714–13719.
[25] Barton-Davis, E.R., Cordier, L., Shoturma, D.I., Leland, S.E. and Sweeney, H.L. (1999) J. Clin. Invest. 104, 375–381.
[26] Gussoni, E., Soneoka, Y., Strickland, C.D., Buzney, E.A., Khan, M.K., Flint, A.F., Kunkel, L.M. and Mulligan, R.C. (1999) Nature 401, 390–394.
[27] Dennis, C.L., Tinsley, J.M., Deconinck, A.E. and Davies, K.E. (1996) Nucleic Acids Res. 24, 1646–1652.
[28] Burton, E.A., Tinsley, J.M., Holzfeind, P.J., Rodrigues, N.R. and Davies, K.E. (1999) Proc. Natl. Acad. Sci. USA 96, 14025–14030.
[29] Gramolini, A.O., Angus, L.M., Schaeffer, L., Burton, E.A., Tinsley, J.M., Davies, K.E., Changeux, J.P. and Jasmin, B.J. (1999) Proc. Natl. Acad. Sci. USA 96, 3223–3227.
[30] Walter, M.C. and Lochmuller, H. (2001) Expert Opin. Invest. Drugs 10, 695–707.
[31] Nakamura, A., Harrod, G.V. and Davies, K.E. (2001) Neuromusc. Disord. 11, 251–259.
[32] Spindler, M., Saupe, K.W., Christe, M.E., Sweeney, H.L., Seidman, C.E., Seidman, J.G. and Ingwall, J.S. (1998) J. Clin. Invest. 101, 1775–1783.
[33] Skrabek, R.Q. and Anderson, J.E. (2001) Muscle Nerve 24, 192–197.
[34] McIntosh, L.M., Granberg, K.E., Briere, K.M. and Anderson, J.E. (1998) NMR Biomed. 11, 1–10.
[35] Dort, J.C., Fan, Y. and McIntye, D.D. (2001) Otolaryngol. Head Neck Surg. 125, 617–622.
[36] Nicholson, J.K., Connelly, J., Lindon, J.C. and Holmes, E. (2002) Nature Rev. Drug Discov. 1, 153–161.
[37] Raamsdonk, L.M., Teusink, B., Broadhurst, D., Zhang, N., Hayes, A., Walsh, M.C., Berden, J.A., Brindle, K.M., Kell, D.B., Rowland, J.J., Westerhoff, H.V., van Dam, K. and Oliver, S.G. (2001) Nature Biotechnol. 19, 45–50.
[38] Gieseler, K., Grisoni, K. and Segalat, L. (2000) Curr. Biol. 10, 1092–1097.